

Collective Behavior Modeling Through Velocity Alignment

by

Jacy Thor Zanussi

A Thesis Submitted in Partial Fulfillment
of the Requirements for the Degree of
Master of Science in Mathematics.

Middle Tennessee State University
March 2019

Thesis Committee:

Dr. Zachariah Sinkala, Chair

Dr. Wandi Ding

Dr. Abdul Khaliq

DEDICATION

This thesis is dedicated to my close friends and family who have given me their support throughout my life and education.

ACKNOWLEDGMENTS

I personally thank Dr. Sinkala for mentoring me over several years in various fields of mathematics, inspiring me to pursue research, and for being a supportive advisor in the process of writing this thesis. I would also like to thank Dr. Khaliq and Dr. Ding for agreeing to be on my thesis committee and for giving me constructive feedback.

ABSTRACT

We construct a model for collective behavior phenomena by undermining the assumption that the rate of change of position equals velocity in the particle Cucker-Smale model for flocking. Conditions for collective behavior are proven and three continuous models for segregation are presented with simulations for two of them. Future avenues of research and a variety of applications such as social science, engineering, and business trends are discussed in the conclusion.

Contents

LIST OF FIGURES	vi
CHAPTER 1: Introduction	1
CHAPTER 2: Extending The Cucker-Smale Model	3
2.1 The Model	5
2.2 Collective Behavior Conditions	5
2.3 Further Results About The Variant Model	9
2.3.1 A Simulation	14
CHAPTER 3: A Model for Segregation	16
3.1 Motivation: Schelling's Segregation Model	16
3.2 The Method of Construction	17
3.3 A Model Using The Gradient	18
3.4 A Segregation Model Derived From Velocity Alignment	21
3.4.1 Simulations Of The First ODE Model	22
3.5 A Second ODE Model	28
3.5.1 Simulations Of The Second ODE Model	28
CHAPTER 4: Concluding Remarks	34
BIBLIOGRAPHY	36
APPENDICES	38
APPENDIX A: THEOREMS	39
APPENDIX B: NOTATION	42

List of Figures

1	On the left, agents are distributed facing random directions at $T = 0$. On the right, a flock of agents at $T = 20$ positioned in a circle of radius 5, facing towards the bottom left, and centered near the origin.	15
2	On the left, the initial distribution of agents for $ q_P = q_N = 0.5$ in the first ODE model in one dimension. 9 agents were dissatisfied. On the right, the end distribution of agents at $T = 20$ for $ q_P = q_N = 0.5$. 0 agents were dissatisfied.	23
3	On the left, the initial Distribution of agents for $ q_P = q_N = 0.6$ in the first ODE model in one dimension. 46 agents were dissatisfied. On the right, the end distribution of agents at $T = 20$ for $ q_P = q_N = 0.6$. 17 agents were dissatisfied.	23
4	On the left, the initial distribution of agents for $ q_P = q_N = 0.7$ in the first ODE model in one dimension. 57 agents were dissatisfied. On the right, the end distribution of agents at $T = 20$ for $ q_P = q_N = 0.7$. 4 agents were dissatisfied.	24
5	On the left, the initial distribution of agents for $ q_P = q_N = 0.8$ in the first ODE model in one dimension. 60 agents were dissatisfied. On the right, the end distribution of agents at $T = 20$ for $ q_P = q_N = 0.8$. 18 agents were dissatisfied.	24
6	On the left, the initial distribution of agents for $ q_P = q_N = 0.9$ in the first ODE model in one dimension. 58 agents were dissatisfied. On the right, the end distribution of Particles at $T = 20$ for $ q_P = q_N = 0.9$. 39 agents were dissatisfied.	25

7	On the left, the initial distribution of agents for $ q_P = q_N = 0.5$ in the first ODE model in two dimensions. 8 agents were dissatisfied. On the right, the end distribution of agents at $T = 20$ for $ q_P = q_N = 0.5$. 0 agents were dissatisfied.	25
8	On the left, the initial distribution of agents for $ q_P = q_N = 0.6$ in the first ODE model in two dimensions. 18 agents were dissatisfied. On the right, the end distribution of agents at $T = 20$ for $ q_P = q_N = 0.6$. 0 agents were dissatisfied.	26
9	On the left, the initial distribution of agents for $ q_P = q_N = 0.7$ in the first ODE model in two dimensions. 26 agents were dissatisfied. On the right, the end distribution of agents at $T = 20$ for $ q_P = q_N = 0.7$. 9 agents were dissatisfied.	26
10	On the left, the initial distribution of agents for $ q_P = q_N = 0.8$ in the first ODE model in two dimensions. 41 agents were dissatisfied. On the right, the end distribution of agents at $T = 20$ for $ q_P = q_N = 0.8$. 15 agents were dissatisfied.	27
11	On the left, the initial distribution of agents for $ q_P = q_N = 0.9$ in the first ODE model in two dimensions. 53 agents were dissatisfied. On the right, the end distribution of agents at $T = 20$ for $ q_P = q_N = 0.9$. 30 agents were dissatisfied.	27
12	On the left, the initial distribution of agents with $ q_P = q_N = 0.5$ in the second ODE model in one dimension. 49 agents were dissatisfied. On the right, the end distribution of agents with $T = 10$. 0 agents were dissatisfied.	29

13	On the left, the initial distribution of agents with $ q_P = q_N = 0.6$ in the second ODE model in one dimension. 105 agents were dissatisfied. On the right, the end distribution of agents with $T = 10$. 0 agents were dissatisfied.	29
14	On the left, the initial distribution of agents with $ q_P = q_N = 0.7$ in the second ODE model in one dimension. 120 agents were dissatisfied. On the right, the end distribution of agents with $T = 10$. 0 agents were dissatisfied.	30
15	On the left, the initial distribution of agents with $ q_P = q_N = 0.8$ in the second ODE model in one dimension. 120 agents were dissatisfied. On the right, the end distribution of agents with $T = 10$. 0 agents were dissatisfied.	30
16	On the left, the initial distribution of agents with $ q_P = q_N = 0.9$ in the second ODE model in one dimension. 120 agents were dissatisfied. On the right, the end distribution of agents with $T = 10$. 0 agents were dissatisfied.	31
17	On the left, the initial distribution of agents with $ q_P = q_N = 0.5$ in the second ODE model in two dimensions. 34 agents were dissatisfied. On the right, the end distribution of agents with $T = 10$. 0 agents were dissatisfied.	31
18	On the left, the initial distribution of agents with $ q_P = q_N = 0.6$ in the second ODE model in two dimensions. 70 agents were dissatisfied. On the right, the end distribution of agents with $T = 10$. 0 agents were dissatisfied.	32

19	On the left, the initial distribution of agents with $ q_P = q_N = 0.7$ in the second ODE model in two dimensions. 111 agents were dissatisfied. On the right, the end distribution of agents with $T = 10$. 0 agents were dissatisfied.	32
20	On the left, the initial distribution of agents with $ q_P = q_N = 0.8$ in the second ODE model in two dimensions. 120 agents were dissatisfied. On the right, the end distribution of agents with $T = 10$. 0 agents were dissatisfied.	33
21	On the left, the initial distribution of agents with $ q_P = q_N = 0.9$ in the second ODE model in two dimensions. 120 agents were dissatisfied. On the right, the end distribution of agents with $T = 10$. 0 agents were dissatisfied.	33

CHAPTER 1

Introduction

Models of flocking find their origins in Reynold's Birdoids, or Boids, created in the 1980's that run off of three rules: Boids align their velocities according to the average velocity of their neighbors, avoid colliding with one another, and attract into groups [1]. In 1995, Vicsek et al. introduced a computational model of "biologically motivated interactions" that exhibited a kinetic phase transition through the spontaneous breaking of rotational symmetry [2]. In 2007, Cucker and Smale reformulated the model found in Vicsek et al. as a system of differential equations and offered rigorous criteria for flocking that verified the speculated phase transition found in Vicsek et al. [3]. Not long after, the particle description of flocking was extended to kinetic and hydrodynamic descriptions to deal with systems with large populations and densities [4]. These systems are currently active areas of mathematical research with new advances in the modern understanding of swarming behavior. For example, the well-posedness of the kinetic description was shown in the weak sense in 2013 [5] and a recent paper proved flocking criteria in the particle and hydrodynamic descriptions for interactions with a limited range [6].

The historical progression from Reynold's and Vicsek's simulations to the mathematical formulas of Cucker and Smale suggests a similar line of reasoning may apply for developing continuous models from a corresponding algorithmic agent-based simulations. As new models become available, more descriptions and analyses arise and the language about the phenomena becomes clearer. Fields such as biology, economics, sociology, politics, and business have relied on agent-based models extensively to develop theories, aid in decision-making, and make predictions [7]. For

example, Schelling's famous model describes how people may segregate by desiring that a percentage of their neighbors are of the same race or characteristic as themselves and by moving around until they satisfy that desire [8]. Hypothetically, segregation may then occur between two groups without people actively avoiding those who are different from themselves. Perhaps some continuous analog to the model exists that offers new perspectives and qualitative information about segregation.

This thesis has two goals: to explore a variation of the Cucker-Smale Model that loosens the geometric restriction of its agents to their group psychology and to show how the velocity alignment equation can afford easily accessible intuition in other collective behavior phenomena by constructing three continuous segregation models. Chapter two explores the Cucker-Smale Model variant and proves theoretical results for collective behavior as well as computational examples. Chapter three shows the creation and simulation of a system of partial differential equations relying on the gradient and of two systems of ordinary differential equations inspired by velocity alignment. The paper concludes with a reflection on its themes and a discussion on future avenues of research theoretical and applied.

CHAPTER 2

Extending The Cucker-Smale Model

For N agents¹ in d spatial dimensions, the Particle Cucker-Smale Model is often written as:

$$\begin{cases} \dot{x}_i = v_i \\ \dot{v}_i = \frac{K}{N} \sum_{j=1}^N \psi(|x_i - x_j|)(v_j - v_i) \end{cases} \quad (1)$$

for initial conditions $x_i(0) = x_{i0} \in \mathbb{R}^d$ and $v_i(0) = v_{i0} \in \mathbb{R}^d$ where $K > 0$ is the coupling constant, $|\cdot|$ represents the Euclidean norm, $\psi : [0, \infty) \rightarrow [0, \infty)$ is a nonincreasing, continuous function, and $x_i : \mathbb{R} \rightarrow \mathbb{R}^d$ and $v_i : \mathbb{R} \rightarrow \mathbb{R}^d$ are functions of time representing the position and velocity of the i th agent respectively. A number of comments are worth mentioning:

1. The first equation says that the rate of change of an agent's position equals its velocity.
2. The second equation says that each particle attempts to align its velocity towards a weighted average of the velocities of its neighbors. Note if the coupling constant K is instead negative, the agents will steer away from the weighted average of the velocities of their neighbors. This causes each agent's weighted average of velocities to deviant significantly and the agents to repel.
3. The function ψ together with the input of $|x_i - x_j|$ represents the tendency of particles to take more influence from nearer neighbors than farther ones. The function ψ is called the "influence function."

¹The word "agent" has been used to replace the more common term "particle" to reflect the context of the models studied in this paper.

4. External forces are negligible.

The first three comments reflect on indispensable assumptions for modeling flocking. The first comment expresses how the geometric and physical aspects of the particles depend on the sociological aspects as perceived through velocity. The second and third comments determine how the sociological and psychological aspects of the individuals depend on the group and how they rely on the geometric and physical aspects of the agents. We refer to $\dot{v}_i = \frac{K}{N} \sum_{j=1}^N \psi(|x_i - x_j|)(v_j - v_i)$ as the "velocity alignment equation."

Velocity alignment states a relationship amongst the agents of the system that manifests as a cooperative activity where every agent eventually achieves the same goal, nearly equal velocities. So, velocity alignment may act as a basic ingredient for modeling a broad variety of social behavior. Introducing a nonconforming agent into the group of conforming ones may then extend the model to a larger class of phenomena. For now, we consider only an extension of the Cucker-Smale model that undermines the first assumption by defining the spatial movement of each agent by $\dot{x}_i = f_i(x, v)$. The extension or variant system loosens the restriction of group orientation and geometry on its sociology, allowing for more abstract models of group behavior.

2.1 The Model

The model proposed in this paper for N agents in d spatial dimensions is stated as follows:

$$\begin{cases} \dot{x}_i = f_i(x, v) \\ \dot{v}_i = \frac{K}{N} \sum_{j=1}^N \psi(|x_i - x_j|)(v_j - v_i) \end{cases} \quad (2)$$

for initial conditions $x_i(0) = x_{i0} \in \mathbb{R}^d$ and $v_i(0) = v_{i0} \in \mathbb{R}^d$ where $K > 0$, $|\cdot|$, ψ , x_i , v_i are defined as in (1) and f_i , called the "movement function," is a function of x and v for each i . We refer to (2) as the "Cucker-Smale Variant." If $f_i(x, v) = v_i$ for each i , the system reduces to the Particle Cucker-Smale Model. The system (2) undermines the first assumption of the Cucker-Smale Model by allowing \dot{x}_i to equal functions other than v_i , or by letting the movement of each agent be governed by more than direction and speed. The second and third assumptions remain unaffected and the fourth assumption may not necessarily hold. The structure of f_i allows one to include external forces on the agents. For example, defining $f_i = v_i - w(x)$ where $w(x)$ represents the affect of wind could model a flock of birds attempting to travel in a windy environment.

2.2 Collective Behavior Conditions

With the Cucker-Smale Variant now defined, conditions in which the agents will align their velocity are now proven. Define the following functions:

$$X(t) = \max_{1 \leq i, j \leq N} |x_i(t) - x_j(t)| \quad (3)$$

$$V(t) = \max_{1 \leq i, j \leq N} |v_i(t) - v_j(t)| \quad (4)$$

$$F(t) = \max_{1 \leq i, j \leq N} |f_i(t) - f_j(t)| \quad (5)$$

Lemma 2.1 *Let f_i be Lipschitz and (x, v) be any solution to the system (2). Then,*

$$\frac{d}{dt}X(t) \leq F(t) \quad (6)$$

$$\frac{d}{dt}V(t) \leq -K\psi(X(t))V(t) \quad (7)$$

where $X(t)$, $V(t)$, and $F(t)$ are defined in (3), (4), and (5) respectively.

Proof: Let $t \geq 0$ and $1 \leq i, j \leq N$. Since $X(t)$ and $F(t)$ are Lipschitz, we have:

$$\frac{1}{2} \frac{d}{dt} |x_i - x_j|^2 = (x_i - x_j) \cdot (\dot{x}_i - \dot{x}_j) \leq X(t)F(t)$$

Integrating from t_0 to t and rearranging terms gives

$$\begin{aligned} \int_{t_0}^t \frac{1}{2} \frac{d}{ds} |x_i(s) - x_j(s)|^2 ds &\leq \int_{t_0}^t X(s)F(s)ds = I \\ \frac{1}{2} [|x_i(t) - x_j(t)|^2 - |x_i(t_0) - x_j(t_0)|^2] &\leq I \\ \frac{1}{2} |x_i(t) - x_j(t)|^2 &\leq \frac{1}{2} |x_i(t_0) - x_j(t_0)|^2 + I \\ &\leq \frac{1}{2} X^2(t_0) + I \end{aligned}$$

Since this last inequality holds for all $t \geq 0$ and $1 \leq i, j \leq N$, we have

$$\frac{1}{2} X^2(t) \leq \frac{1}{2} X^2(t_0) + I$$

Subtracting and rewriting the integral gives us:

$$\begin{aligned} \frac{1}{2} (X^2(t) - X^2(t_0)) &\leq \int_{t_0}^t X(s)F(s)ds \\ \int_{t_0}^t \frac{d}{ds} \left(\frac{1}{2} X^2(s) \right) ds &\leq \int_{t_0}^t X(s)F(s)ds \\ \int_{t_0}^t X(s) \left(\frac{d}{ds} X(s) \right) ds &\leq \int_{t_0}^t X(s)F(s)ds \end{aligned}$$

$$\int_{t_0}^t X(s) \left[\frac{d}{dt} X(s) - F(s) \right] ds \leq 0$$

Since $X(s) \geq 0$ for all $s \geq 0$, The above inequality holds true only when $\frac{d}{ds} X(s) \leq F(s)$ for all $s \geq 0$.

The inequality (7) has been proven in other works and the proof remains unchanged for the Cucker-Smale Variant. Ha and Lie prove the inequality for example [10]. See Appendix A for a proof. \square

$\frac{d}{dt} V(t) < -K\psi(X(t))V(t)$ does not guarantee the convergence of $V(t)$ to 0 unless the product $\psi(X(t))V(t)$ grows sufficiently fast compared to the dispersion of agents. If $X(t) \leq r$ for some constant $r \in \mathbb{R}$, then $\frac{d}{dt} V(t) \leq -K\psi(r)V(t)$ and a special case of Grönwall's Inequality in differential form, found in Appendix A, applies so that flocking occurs. The following theorem offers a criteria reminiscent of other works:

Theorem 2.2 *If (x, v) is a solution the system of equations in (2) where f_i is Lipschitz that also satisfies:*

$$V(0) < \frac{K}{C} \int_{X(0)}^{\infty} \psi(s) ds$$

and

$$F(t) \leq CV(t)$$

for $t \geq 0$ and for some $C > 0$, then

$$V(t) \leq V(0)e^{-K\psi(r)t} \quad \forall t \geq 0$$

where r is implicitly defined by $V(0) = \frac{K}{C} \int_{X(0)}^r \psi(s) ds$ and K and ψ and defined as in Equation (2).

Proof: Define $\epsilon = V(t) + \frac{K}{C} \int_{X(0)}^{X(t)} \psi(s)ds$. Taking the derivative with respect to t and using Lemma 2.1 yields

$$\begin{aligned} \frac{d}{dt}\epsilon(t) &= \frac{d}{dt}V(t) + \frac{K}{C}\psi(X(t))\frac{d}{dt}X(t) \\ &\leq -K\psi(X(t))V(t) + \frac{K}{C}\psi(X(t))F(t) \\ &\leq -K\psi(X(t))V(t) + K\psi(X(t))V(t) = 0 \end{aligned}$$

So, $\epsilon(t)$ is a decreasing function over $[0, \infty)$, i.e. $V(t) + \frac{K}{C} \int_{X(0)}^{X(t)} \psi(s)ds \leq V(0)$. By the assumption of the first inequality, there exists some $r > X(0)$ such that $V(0) = \frac{K}{C} \int_{X(0)}^r \psi(s)ds$. So,

$$0 < V(t) \leq \frac{K}{C} \int_{X(0)}^r \psi(s)ds - \frac{K}{C} \int_{X(0)}^{X(t)} \psi(s)ds = \frac{K}{C} \int_{X(t)}^r \psi(s)ds$$

Thus, $X(t) \leq r$, which means that $X(t)$ is bounded above by some constant. By the second part of Lemma 2.1, we have:

$$\frac{d}{dt}V(t) \leq -K\psi(X(t))V(t) \leq -K\psi(r)V(t) \tag{8}$$

The result follows from applying the special case of Grönwall's Inequality in differential form found in Appendix A. \square

If the system of equations (2) achieves collective behavior for ψ for a solution with initial conditions satisfying Theorem 2.2, then the system obtained by replacing $\psi(x)$ with $\phi(x)$ also achieves collective behavior for any function $\phi : [0, \infty) \rightarrow [0, \infty)$ such that $0 < \phi(x) \leq \psi(x) \forall x > 0$. This follows from observing in (8) that $-K\psi(r)V(t) \leq -K\phi(r)V(t)$. Thus, $V(t) \leq V(0)e^{-K\phi(r)t}$ if the prior conditions are met. The argument implies that an upper bound on $X(t)$ almost suffices to guarantee flocking by itself.

2.3 Further Results About The Variant Model

With the following lemmas and theorems, mechanisms for analyzing the orientation of a group of particles satisfying the Cucker-Smale Variant, (2), are proven. The first lemma concerns representing (2) by centering it at the origin. Define the "Centered Cucker-Smale Variant" as

$$\begin{cases} \dot{x}_i = f_i - \bar{f} \\ \dot{v}_i = \frac{K}{N} \sum_{j=1}^N \psi(|x_i - x_j|)(v_j - v_i) \end{cases} \quad (9)$$

Lemma 2.3 *If (x, v) solves the Centered Cucker-Smale Variant, (9), then the center of position, $\bar{x}(t) = \frac{1}{N} \sum_{j=1}^N x_j(t)$, remains constant through time.*

Proof: Since the derivative of a function equals 0 if and only if that function is constant, it suffices to show that $\frac{d}{dt}\bar{x}(t) = \dot{\bar{x}}(t) = 0$.

$$\begin{aligned} \frac{d}{dt}\bar{x}(t) &= \frac{d}{dt} \frac{1}{N} \sum_{j=1}^N x_j(t) \\ &= \frac{1}{N} \sum_{j=1}^N \frac{d}{dt} x_j(t) \\ &= \frac{1}{N} \left(\sum_{j=1}^N f_j(t) - \bar{f} \right) \\ &= \frac{1}{N} \sum_{j=1}^N f_j(t) - \frac{1}{N} \sum_{j=1}^N \bar{f} \\ &= \bar{f} - \bar{f} = 0 \end{aligned}$$

Thus, \bar{x} is constant. \square

For an alternative proof, note that $\bar{f} = \frac{1}{N} \sum_{j=1}^N f_j = \sum_{j=1}^N (\bar{f} + \dot{x}_i) = \bar{f} + \dot{\bar{x}}$. So, $\bar{f} = \bar{f} + \dot{\bar{x}}$ and hence $\dot{\bar{x}} = 0$. The next lemma proves that the orientation of positions for the solutions to (2) and (9) are equal assuming the initial conditions are equal.

Lemma 2.4 *If (u, w) is a solution to the system (9), and (x, v) is a solution to the system (2) where both have the same initial conditions $u(0) = x(0) = x_0 = u_0$ and $w(0) = v(0) = v_0 = w_0$, then $x_i - \bar{x} = u_i - \bar{u}$ for all i .*

Proof: Let $t \geq 0$. Let (x, v) solve the system (2). The relative position of particle i within the flock at time t is given by $x_i(t) - \bar{x}(t)$. Likewise, if (u, v) solves the system (6), the relative position of particle i equals $u_i(t) - \bar{u}(t)$. We begin by showing that the derivatives of relative positions are equal. In other words, we show

$\frac{d}{dt}(x_i(t) - \bar{x}(t)) = \frac{d}{dt}(u_i(t) - \bar{u}(t))$. By the Lemma 2.3, $\bar{u}(t)$ is constant throughout time. So,

$$\begin{aligned} & \frac{d}{dt}(x_i(t) - \bar{x}(t) - u_i(t) - \bar{u}(t)) \\ &= (\dot{x}_i(t) - \dot{\bar{x}}(t) - \dot{u}_i(t) - \dot{\bar{u}}(t)) \\ &= f_i(t) - \bar{f}(t) - (f_i(t) - \bar{f}(t)) = 0 \end{aligned}$$

Note that, since (x, v) and (u, w) satisfy their respective systems over the same initial conditions, that $\bar{x}(0) = \bar{u}(0)$. Rearranging terms and integrating from 0 to t gives

$$\begin{aligned} \int_0^t \dot{x}_i(s) - \dot{\bar{x}}(s) ds &= \int_0^t \dot{u}_i(s) - \dot{\bar{u}}(s) ds \\ x_i(t) - \bar{x}(t) - (x_i(0) - \bar{x}(0)) &= u_i(t) - \bar{u}(t) - (u_i(0) - \bar{u}(0)) \\ x_i(t) - \bar{x}(t) &= u_i(t) - \bar{u}(t) - (u_i(0) - \bar{u}(0)) + (x_i(0) - \bar{x}(0)) \\ x_i(t) - \bar{x}(t) &= u_i(t) - \bar{u}(t) - (u_0 - \bar{u}_0) + (x_0 - \bar{x}_0) \end{aligned}$$

$$x_i(t) - \bar{x}(t) = u_i(t) - \bar{u}(t) \quad (10)$$

Equation (10) gives several fruitful equalities.

Corollary 2.5 *If (u, w) is a solution to the system (9), and (x, v) is a solution to the system (2) where both have the same initial conditions $u(0) = x(0) = x_0 = u_0$ and $w(0) = v(0) = v_0 = w_0$, then the following identities hold for all $t \geq 0$ and for all i .*

1. $x_i(t) - u_i(t) = \bar{x}(t) - \bar{u}(t)$
2. $x_i(t) + \bar{u}(t) = u_i(t) + \bar{x}(t)$
3. $x_i(t) = u_i(t) + \bar{x}(t) - \bar{u}(t) = u_i(t) + \int_0^t \dot{\bar{x}}(s) ds$
4. $x_i(t) = u_i(t) + \int_0^t \bar{f}(s) ds$
5. $u_i(t) = x_i(t) - \int_0^t \bar{f}(s) ds$

Remark: Identities 4 and 5 yield explicit solutions to (2) or (9). For example, if (u, w) solves (9), then $(u + \int_0^t \bar{f}(s) ds, w)$ will solve (2). Likewise, if (x, v) solves (2), then $x - \int_0^t \bar{f}(s) ds$. Since f_i is often explicitly defined, Corollary 2.5 gives an easy method of constructing explicit solutions to (2) given a solution to (9) and vice versa.

The next theorem shows a result for a specific definition of f_i .

Theorem 2.6 *Let $f_i(t) = \alpha(d_i(t) - x_i(t))$ for $\alpha > 0$ be a differentiable function where $d_i(t) = c(t) + \bar{x}(t)$.*

1. *If (x, y) solves (9) with $f_i = \alpha(d_i - x_i)$.*
2. $\bar{d} = \bar{x}$
3. $\lim_{t \rightarrow \infty} d'_{ij}(t) = 0$

4. If $\lim_{t \rightarrow \infty} \alpha \int_0^t e^{\alpha s} d'_{ij}(s) ds$ exists or tends to positive or negative infinity.

then $x_i(t) \rightarrow d_i(t)$ as $t \rightarrow \infty$.

Proof. Note that $\bar{f} = \alpha(\bar{d} - \bar{x}) = 0$ by assumption and if $\bar{x}_i = 0$ if and only if $d_i = x_i$. If \dot{x}_i is a nonzero function, then we must show that $\lim_{t \rightarrow \infty} \dot{x}_i(t) = 0$. This is sufficient to show that $x_i(t) \rightarrow d_i(t)$ as $t \rightarrow \infty$. Consider $x_{ij}(t)$, the j th component of agent i . The differential equation

$$x'_{ij}(t) = \alpha(d_{ij}(t) - x_{ij}(t)) - \bar{f} = \alpha(d_{ij}(t) - x_{ij}(t))$$

has a known solution. Using integration by parts on the solution and simplifying gives

$$\begin{aligned} x_{ij}(t) &= \alpha e^{-\alpha t} \int_0^t e^{\alpha s} d_{ij}(s) ds + C e^{-\alpha t} \\ &= \alpha e^{-\alpha t} \left(\frac{e^{\alpha t}}{\alpha} d_{ij}(t) - \int_0^t e^{\alpha s} d'_{ij}(s) ds \right) + C e^{-\alpha t} \\ &= d_{ij}(t) - \alpha e^{-\alpha t} \int_0^t e^{\alpha s} d'_{ij}(s) ds + C e^{-\alpha t} \end{aligned}$$

Since $\lim_{t \rightarrow \infty} C e^{-\alpha t} = 0$, if $\lim_{t \rightarrow \infty} e^{-\alpha t} \alpha \int_0^t e^{\alpha s} d'_{ij}(s) ds = 0$, then $\lim_{t \rightarrow \infty} x_{ij}(t) = \lim_{t \rightarrow \infty} d_{ij}(t)$.

Consider the limit

$$L = \lim_{t \rightarrow \infty} e^{-\alpha t} \alpha \int_0^t e^{\alpha s} d'_{ij}(s) ds = \lim_{t \rightarrow \infty} \frac{\alpha \int_0^t e^{\alpha s} d'_{ij}(s) ds}{e^{\alpha t}} \quad (11)$$

If $\alpha \int_0^t e^{\alpha s} d'_{ij}(s) ds$ is bounded or tends to 0, then $L = 0$ since $\lim_{t \rightarrow \infty} e^{-\alpha t} = 0$. If $\alpha \int_0^t e^{\alpha s} d'_{ij}(s) ds$ tends to positive or negative infinity, we may use L'Hôpital's rule to obtain

$$\lim_{t \rightarrow \infty} \frac{\alpha \int_0^t e^{\alpha s} d'_{ij}(s) ds}{e^{\alpha t}} = \lim_{t \rightarrow \infty} \frac{\alpha e^{\alpha t} d'_{ij}(t)}{\alpha e^{\alpha t}} = \lim_{t \rightarrow \infty} d'_{ij}(t)$$

Since $\lim_{t \rightarrow \infty} d'_{ij}(t) = 0$ by assumption, the limit equals 0. Thus, $x_{ij}(t) \rightarrow d_{ij}(t)$ as $t \rightarrow \infty$. Since convergence holds for an arbitrary component of $x_i(t)$, $x_i(t)$ converges component-wise to $d_i(t)$ in the Euclidean norm for any arbitrary agent i .

□

Since (x, y) solves (9), then if we define u by letting $u_i(t) = x_i(t) - \int_0^t \bar{f}(s) ds$ for all i , we have a solution to the corresponding system (2).

Theorem 2.7 *If the following conditions hold*

1. (x, v) solves (2) with $f_i = \alpha(d_i - x_i)$ defined as in Theorem 2.6.
2. $\lim_{t \rightarrow \infty} \alpha \int_0^t d'_{ij}(s) ds$ exists or tends to positive or negative infinity.
3. $\lim_{t \rightarrow \infty} d'_{ij}(t) = 0$ where d_{ij} is the j th component of agent i .

then $x_i(t) \rightarrow d_i(t)$ as $t \rightarrow \infty$.

Proof. Note that $\bar{f} = \alpha(\bar{d} - \bar{x}) = 0$ by assumption and if $\bar{x}_i = 0$ if and only if $d_i = x_i$. If \dot{x}_i is a nonzero function, then we must show that $\lim_{t \rightarrow \infty} \dot{x}_i(t) = 0$, thereby showing that $x_i(t) \rightarrow d_i(t)$ as $t \rightarrow \infty$. Consider the j th component of agent i , $x_{ij}(t)$.

We have

$$x'_{ij}(t) = \alpha(d_{ij}(t) - x_{ij}(t)) - \bar{f} = \alpha(d_{ij}(t) - x_{ij}(t))$$

which has a known solution. Using integration by parts on that solution and simplifying gives

$$\begin{aligned} x_{ij}(t) &= \alpha e^{-\alpha t} \int_0^t e^{\alpha s} d_{ij}(s) ds + C e^{-\alpha t} \\ &= \alpha e^{-\alpha t} \left(\frac{e^{\alpha t}}{\alpha} d_{ij}(t) - \int_0^t e^{\alpha s} d'_{ij}(s) ds \right) + C e^{-\alpha t} \\ &= d_{ij}(t) - \alpha e^{-\alpha t} \int_0^t e^{\alpha s} d'_{ij}(s) ds + C e^{-\alpha t} \end{aligned}$$

Since $\lim_{t \rightarrow \infty} C e^{-\alpha t} = 0$, if $e^{-\alpha t} \alpha \int_0^t e^{\alpha s} d'_{ij}(s) ds$ tends to 0, then $x_{ij}(t)$ tends to $d_{ij}(t)$.

Consider the limit

$$L = \lim_{t \rightarrow \infty} e^{-\alpha t} \alpha \int_0^t e^{\alpha s} d'_{ij}(s) ds = \lim_{t \rightarrow \infty} \frac{\alpha \int_0^t e^{\alpha s} d'_{ij}(s) ds}{e^{\alpha t}} \quad (12)$$

If $\alpha \int_0^t e^{\alpha s} d'_{ij}(s) ds$ is bounded or tends to 0, then $L = 0$ since $\lim_{t \rightarrow \infty} e^{-\alpha t} = 0$. If $\alpha \int_0^t e^{\alpha s} d'_{ij}(s) ds$ tends to positive or negative infinity, we may use L'Hôpital's rule to obtain

$$\lim_{t \rightarrow \infty} \frac{\alpha \int_0^t e^{\alpha s} d'_{ij}(s) ds}{e^{\alpha t}} = \lim_{t \rightarrow \infty} \frac{\alpha e^{\alpha t} d'_{ij}(t)}{\alpha e^{\alpha t}} = \lim_{t \rightarrow \infty} d'_{ij}(t)$$

Since $\lim_{t \rightarrow \infty} d'_{ij}(t) = 0$ by assumption, the limit equals 0. Thus, $x_{ij}(t) \rightarrow d_{ij}(t)$ as $t \rightarrow \infty$. Since convergence holds for an arbitrary component of $x_i(t)$, $x_i(t)$ converges component-wise to $d_i(t)$ in the Euclidean norm for any arbitrary agent i . \square

2.3.1 A Simulation

Theorem 2.6 has also been verified computationally for 15 agents with initial conditions x_{i0} and v_{i0} randomly uniformly dispersed over the square

$[-5, 5] \times [-5, 5]$ with $\psi(r) = \frac{1}{(1+r^2)^\beta}$ with $\beta = 0.25$. d_i was chosen so that each agent assumed a point on a circle of radius 5 centered at the center of position of the

initial distribution of agents. Each agent was represented by an arrow pointing in the direction of its velocity and positioned at the agent's position. The system was solved using a fourth-order Runge-Kutta method with a time step of $h = 0.01$ for 2000 iterations, which corresponds to the stop time $T = 20$.

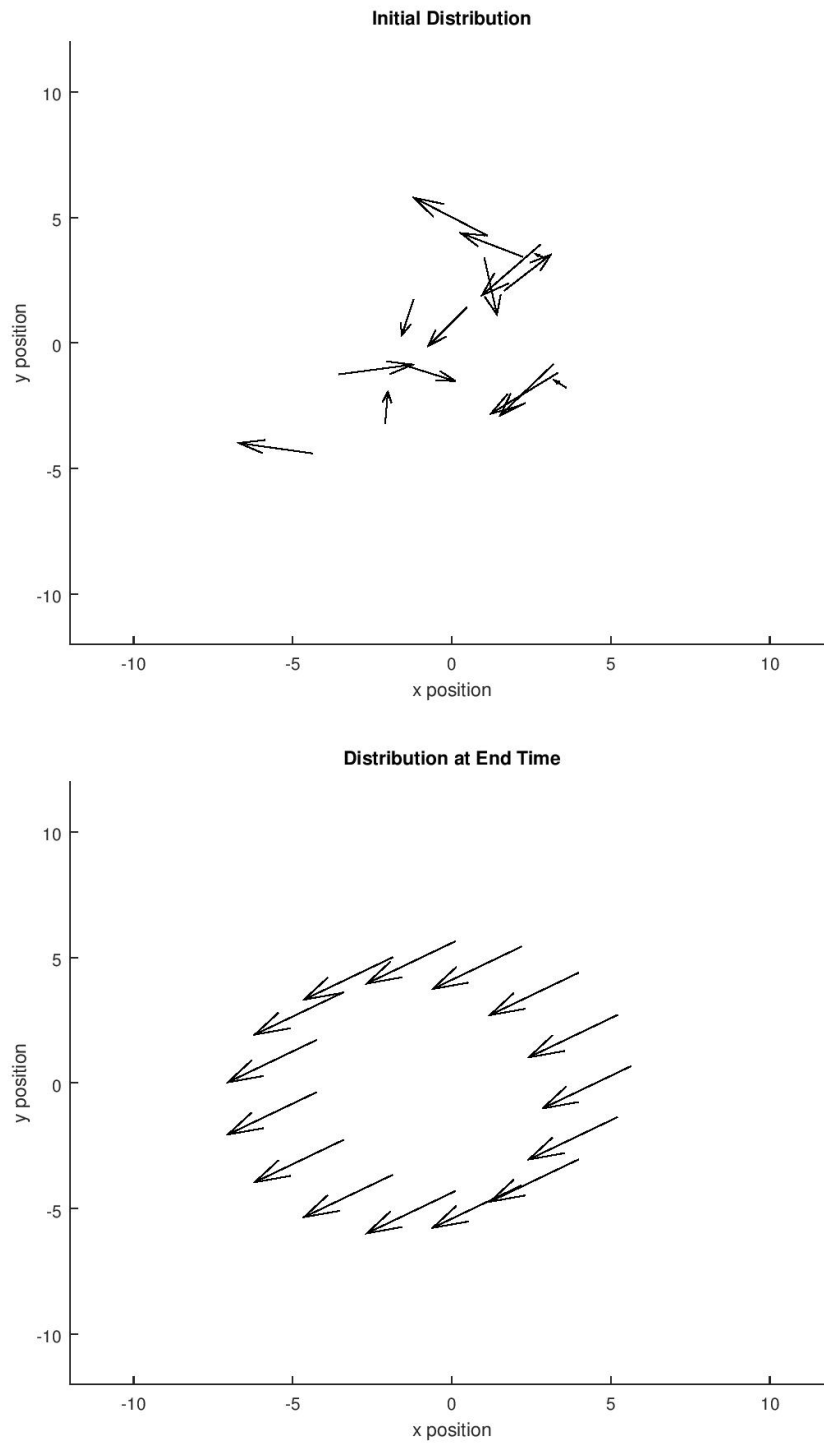


Figure 1: On the left, agents are distributed facing random directions at $T = 0$. On the right, a flock of agents at $T = 20$ positioned in a circle of radius 5, facing towards the bottom left, and centered near the origin.

CHAPTER 3

A Model for Segregation

3.1 Motivation: Schelling's Segregation Model

In 1971, Schelling created an agent-based model for self-segregation based on simple rules [8]. N agents are attributed one of two qualities and are then randomly distributed on a line or two-dimensional grid. Each agent desires that a percentage of its nearest k neighbors are the same quality as itself. Given this preference, each agent then moves with some predetermined rule until satisfied. Explicitly, the assumptions may be stated as follows:

1. Each agent has a quality that falls into one of two categories.
2. Each agent is satisfied only when some percentage of its neighbors are of the same quality as itself.
3. Each agent attempts to find the nearest location, whether by random movement or not, that satisfies the requirement in assumption 2 with a limitation on the particle's movement speed. Once the agent finds a suitable location, it stops moving.

The remainder of this chapter aims to construct models reminiscent of Schelling's segregation. Three are constructed: one relies on gradient flow as a system of PDE; the others resemble the Cucker-Smale model.

3.2 The Method of Construction

The goal is to extend the model above to a spatial and temporal continuum. One of the main difficulties in the construction of this continuous model lies in how the discrete model uses natural, definitive algorithms to induce intended activity.

Translating the assumptions and algorithms of Schelling's model rests in the construction of several functions that replace those algorithms. Our construction begins with defining the following:

1. Assign each i agent a nonzero constant, predetermined quality $q_i \in [-1, 1]$ and a position $x_i \in \mathbb{R}^d$. For simplicity, assume that $|q_i|$ corresponds to the threshold of satisfaction for agent i . The parity of q_i determines the agent's quality. So, we say the agent i has positive parity if $q_i > 0$ and that an agent j has negative parity if $q_j < 0$.
2. Assign each agent a non-increasing, non-negative real-valued influence function, ψ_i governing its perception of neighbors by placing preference on its nearest neighbors to farther ones.²

3. Assign each agent a function that determines its sense of similarity, ϕ_i , that

²The influence function represents a few distinct phenomena. For example, the influence function ψ in the Cucker-Smale model represents agent i 's perception of agent j based on the position of j relative to i . An alternative interpretation could be that ψ represents how the presence of agent j affects agent i . Both scenarios are important in modeling group dynamics: the particle i can be completely receptive or non-receptive of the presence of agent j and vice versa. Such an asymmetry suggests that each agent should have two influence functions governing perception and presence, however, we often assume perfect perception for simplicity. If every agent has the same perception function, we may write $\psi_i = \psi$ without any ambiguity.

allows it to identify others as similar. An intuition choice of ϕ_i would be a characteristic function.

4. Construct the cost function $C : \mathbb{R}^d \times \mathbb{R} \rightarrow [0, 1]$ that takes the position and quality of agent i to the ratio of total influence on i from particles similar to i to the total influence on i from all agents. Mathematically, this corresponds to

$$C(x_i, q_i) = \frac{\text{Similar Influence}}{\text{Total Influence}} = \frac{\sum_{j=1}^N \psi(|x_i - x_j|) \phi(|q_i - q_j|)}{\sum_{j=1}^N \psi(|x_i - x_j|)}$$

5. Construct a function that determines action or movement for the i th agent according to its satisfaction. In the discrete case, we let $\chi_{|q_i|}$ signify the characteristic function on \mathbb{R} that equals 1 over $[0, |q_i|]$ and 0 elsewhere. For smoothness, we replace this function with a suitable compactly supported infinitely differentiable function $\Lambda_{|q_i|}$ that is approximately 1 over $[0, |q_i|]$ and 0 elsewhere.
6. Finally, construct the movement function $\dot{x}_i = f_i$.

With these functions replacing the algorithms of the Schelling model, we proceed in a straight forward way to produce three new segregation models. A natural procedure for movement arises from recognizing the gradient operator in \mathbb{R}^d points each agent in the direction of greatest ascent. Another natural sense of movement arises from using the Cucker-Smale velocity alignment term to move similar agents together according to the cost function.

3.3 A Model Using The Gradient

Let $x_i \in \mathbb{R}^d$ and $q_i \in [-1, 1]$ where $q_i \neq 0$ be the quality of agent i . Since each agent has an assigned nonzero quality q_i between -1 and 1 , let the indices $1 < i < k$

represent the positive agents and $k + 1 \leq j \leq n$ represent the negative ones. Define the influence function $\psi_i : \mathbb{R}^d \rightarrow \mathbb{R}^+$ for each i agent by

$$\psi_i(x) = \frac{1}{(1 + |x - x_i|^2)^\beta}$$

Define the similarity function $\phi : \mathbb{R} \rightarrow \mathbb{R}$ as

$$\phi(r) = \chi_{[0,1]}(r) = \begin{cases} 1 & r \in [0, 1] \\ 0 & r \notin [0, 1] \end{cases}$$

Note that $\phi(q_i q_j) = 1$ if $q_i q_j > 0$ and $\phi(q_i q_j) = 0$ if $q_i q_j < 0$. This corresponds to the notion that two particles are of the same quality if their signs agree. For any agent with positive parity, the influence on particle i from agents of similar parity would simplify to $P(x_i) = \sum_{j=1}^k \psi(|x_i - x_j|) \phi_j(x_i)$. We may rewrite P for any agent of positive parity located at x as $P(x) = \sum_{j=1}^k \psi(|x_i - x_j|) \phi_j(x)$. Likewise, $N(x) = \sum_{j=k+1}^n \psi(|x - x_j|) \phi_j(x)$ represents negative influence at location x and $P(x) + N(x)$ represents the total influence on location x . We have the following cost functions:

$$C_p(x) = \frac{P(x)}{P(x) + N(x)}; \quad C_N(x) = \frac{N(x)}{P(x) + N(x)}$$

Finally, let $\Lambda_{|q_i|}(r) = e^{\frac{-1}{c(|q_i|^2 - r^2)}} \chi_{|q_i|}(r)$, a smooth approximation to the characteristic function $\chi_{|q_i|}(r)$ for $r \in [0, \infty)$ according to the parameter c , be the movement function described in step 5.

We want each agent to move in the direction of greatest ascent on its cost function until it finds the closest location of highest satisfaction or until the agent satisfies its

threshold. A feasible system for this scenario would be

$$\begin{aligned}\frac{\partial}{\partial t}x_i &= \alpha_i \nabla_x C_P(x_i) \Lambda_{|q_i|}(C_P(x_i)) \quad 1 \leq i \leq k \\ \frac{\partial}{\partial t}x_j &= \alpha_j \nabla_x C_N(x_j) \Lambda_{|q_j|}(C_N(x_j)) \quad k+1 \leq j \leq N\end{aligned}\tag{13}$$

For $\alpha_i, \alpha_j > 0$ determining the speed at which the agents settle. Equivalently, since $C_P + C_N = 1$, we can substitute $C_N = 1 - C_P$ to obtain

$$\begin{aligned}\frac{\partial}{\partial t}x_i &= \alpha_i \nabla_x C_P(x_i) \Lambda_{|q_i|}(C_P(x_i)) \quad 1 \leq i \leq k \\ \frac{\partial}{\partial t}x_j &= -\alpha_j \nabla_x C_P(x_j) \Lambda_{|q_j|}(1 - C_P(x_j)) \quad k+1 \leq j \leq N\end{aligned}\tag{14}$$

The system (14) will be called the ”PDE Model” or ”Gradient Model.” The PDE Model will be simulated in future work, but a few facts are known about the PDE Model due to the nature of gradient flow.

1. Since the gradient finds local max and min values, agents of one parity can become stuck between agents of another parity causing certain agents to become stuck and dissatisfied.
2. In the cost function, each agent takes its own presence into consideration. Thus, if the agents are not place in an enclosure, ones along the outside of the initial distribution of agents will disperse until satisfied. The positions of the agents then stay bounded in time since the influence of any agent j on agent i decreases as the distance between i and j increases while the influence of i on itself stays constant.
3. If the boundaries are closed off so that no agent can leave an enclosed region and if the agents have a sufficiently high threshold, then some agents will tend toward the outskirts of the enclosure.

3.4 A Segregation Model Derived From Velocity Alignment

When specific conditions are met for solutions of the Particle Cucker-Smale Model, the velocity alignment equation causes $V(t) = \max_{1 \leq i, j \leq N} |v_i(t) - v_j(t)|$ to tend to 0 as t increases, resulting in every agent's velocity to tend to the same vector v . Also note that if the coupling constant K is negative, the velocities will tend away from each other and the agents repel. With these two observations in mind, we can construct another model of self-segregation. Assume again that each agent has the quality $q_i \in [-1, 1]$ with $q_i \neq 0$. Define the influence function, similarity function, cost function, and movement functions as found in the gradient model. The weighted sum of the differences, $x_j - x_i$, will determine the direction that agent i should tend toward given the influence of agent j . Each difference would have a weight attributed to it based on the influence, similarity, and movement functions. Since the velocity alignment term in the Cucker-Smale model forces $V(t)$ to tend towards 0 as t approaches infinity when flocking occurs, we recognize that the model just stated will result in all agents collapsing into a single point. To remedy this, introduce the factor μ such that $\mu(r) = r^{1/(2l-1)} \approx 1$ for $r > 0$, $\mu(r) = r^{1/(2l-1)} \approx 0$ for $r = 0$, and $\mu(r) = r^{1/(2l-1)} \approx -1$ for $r < 0$ for sufficiently large value of $l \in \mathbb{Z}^+$. The factor $\mu(C(x_i) - C(x_j))$ introduces the assumption that each agent moves towards agents with a lower satisfaction than themselves in an attempt to fill in low-cost space.

For N agents, we have the following system:

$$\dot{x}_i = \alpha_i \left(\sum_{j=1}^N \psi(|x_i - x_j|) \mu(C(x_i) - C(x_j)) (x_j - x_i) \right) \Lambda_{|q_i|}(C(x_i))$$

For the initial conditions $x_i(0) = x_{i0} \in \mathbb{R}^d$ and $q_i(0) = q_{i0} \in \mathbb{R}$. For f nonnegative and decreasing.

3.4.1 Simulations Of The First ODE Model

For an example of the ODE model applying velocity alignment, we ran a 1-dimensional simulation in Matlab using a Fourth-Order Runge-Kutta method. 60 agents were assigned the same threshold value and k agents were assigned positive parity. Positive parity agents are represented as blue circles and negative parity agents are likewise represented by red circles. The positions were randomly uniformly distributed over the interval $[-5, 5]$. For an arbitrary particle (x, q) , we defined the following:

$$\psi(x) = \frac{1}{(1 + |x|^2)^\beta}$$

$$S(x, q) = \sum_{j=1}^n \psi(|x - x_j|) \chi_{[0, \infty)}(qq_j); \quad T(x) = \sum_{j=1}^n \psi(|x - x_j|);$$

$$C(x, q) = \frac{S}{T} \quad x \in \mathbb{R}^d, \quad q \in \mathbb{R}$$

$$\chi_{|q_i|}(r) \approx \Lambda_{|q_i|}(r) = \begin{cases} e^{-\frac{1}{c(|q_i|^2 - r^2)}} & 0 < r < |q_i| \\ 0 & r > |q_i| \end{cases} \quad c > 0$$

$$\mu(r) = r^{1/(2l-1)};$$

We assume that $\alpha_i = a_j$ for all i, j . Denote the thresholds for positive parity agents by $|q_P|$ and the thresholds for negative parity agents by $|q_N|$. The following parameters were chosen: $N = 60$ agents with $k = 30$ positive and negative agents, time $T = 20$, step size for time of $h = 0.01$, $\alpha = 1$, $t = 2$, $\beta = 2$, $l = 1000$, and $c = 1000000$.

Two dimensional simulations were run using the same parameters where the agents were initially randomly uniformly distributed over the square $[-5, 5] \times [-5, 5]$. Only the thresholds, $|q_P| = |q_N|$, were varied and the initial distribution of particles was randomized each simulation as before.

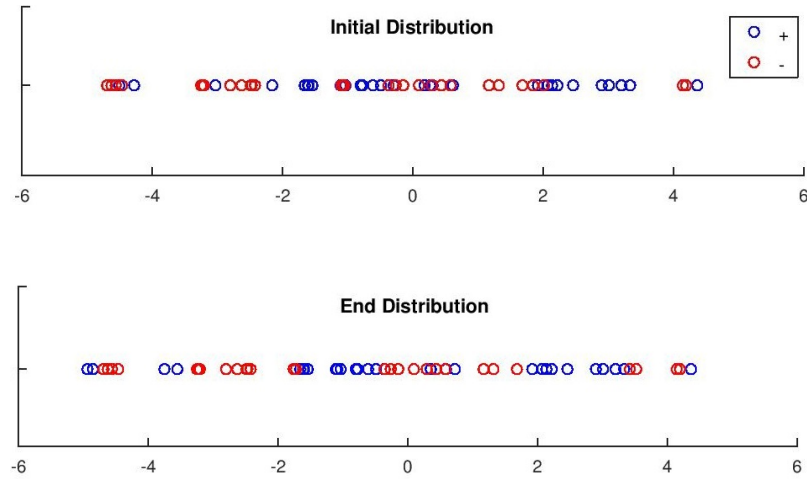


Figure 2: On the left, the initial distribution of agents for $|q_P| = |q_N| = 0.5$ in the first ODE model in one dimension. 9 agents were dissatisfied. On the right, the end distribution of agents at $T = 20$ for $|q_P| = |q_N| = 0.5$. 0 agents were dissatisfied.

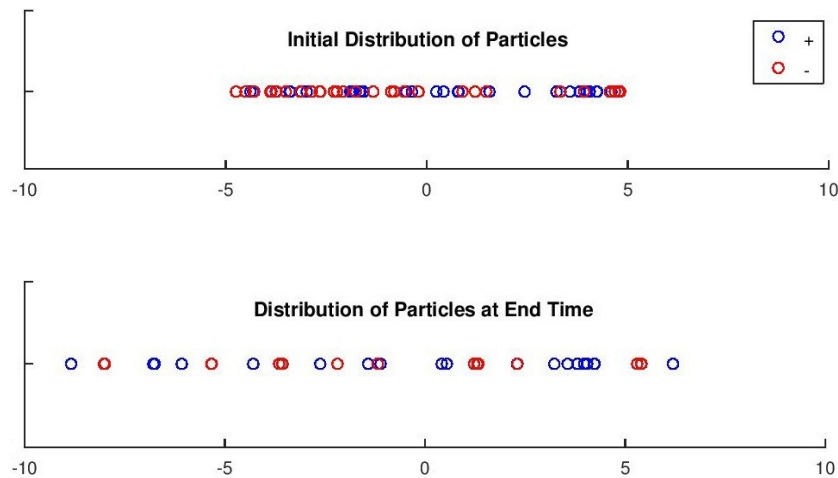


Figure 3: On the left, the initial Distribution of agents for $|q_P| = |q_N| = 0.6$ in the first ODE model in one dimension. 46 agents were dissatisfied. On the right, the end distribution of agents at $T = 20$ for $|q_P| = |q_N| = 0.6$. 17 agents were dissatisfied.

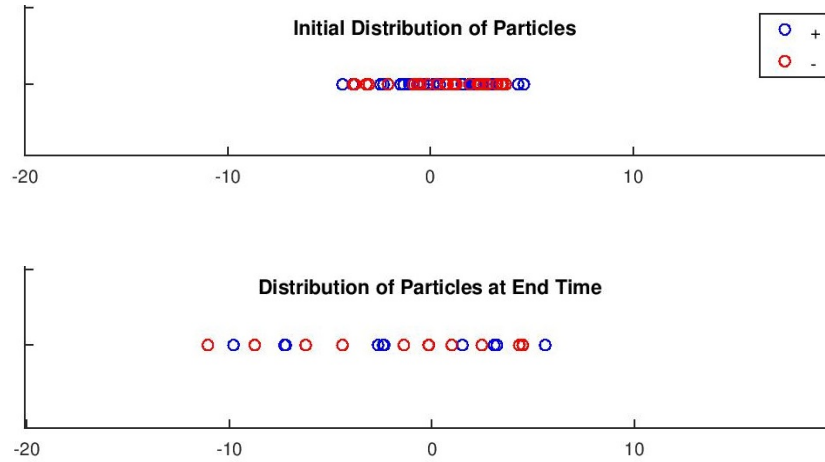


Figure 4: On the left, the initial distribution of agents for $|q_P| = |q_N| = 0.7$ in the first ODE model in one dimension. 57 agents were dissatisfied. On the right, the end distribution of agents at $T = 20$ for $|q_P| = |q_N| = 0.7$. 4 agents were dissatisfied.

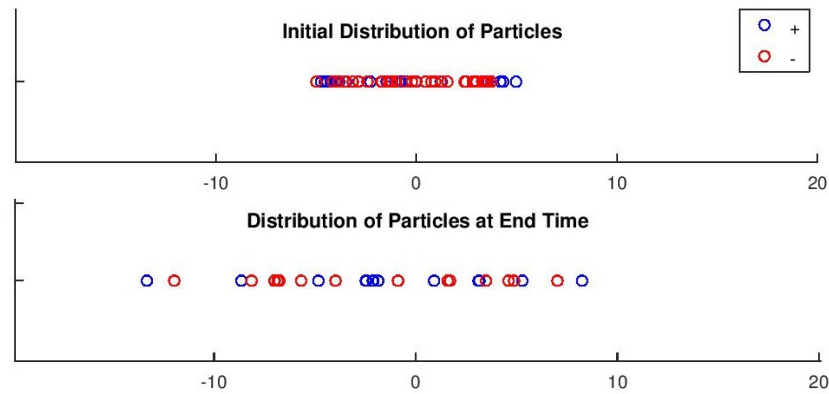


Figure 5: On the left, the initial distribution of agents for $|q_P| = |q_N| = 0.8$ in the first ODE model in one dimension. 60 agents were dissatisfied. On the right, the end distribution of agents at $T = 20$ for $|q_P| = |q_N| = 0.8$. 18 agents were dissatisfied.

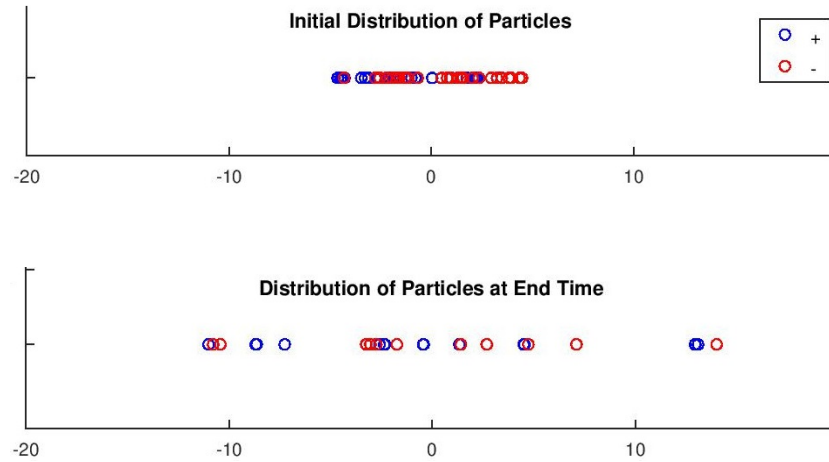


Figure 6: On the left, the initial distribution of agents for $|q_P| = |q_N| = 0.9$ in the first ODE model in one dimension. 58 agents were dissatisfied. On the right, the end distribution of Particles at $T = 20$ for $|q_P| = |q_N| = 0.9$. 39 agents were dissatisfied.

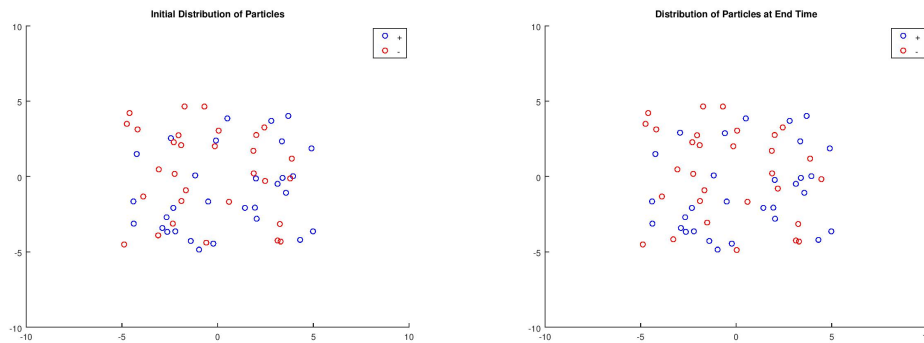


Figure 7: On the left, the initial distribution of agents for $|q_P| = |q_N| = 0.5$ in the first ODE model in two dimensions. 8 agents were dissatisfied. On the right, the end distribution of agents at $T = 20$ for $|q_P| = |q_N| = 0.5$. 0 agents were dissatisfied.

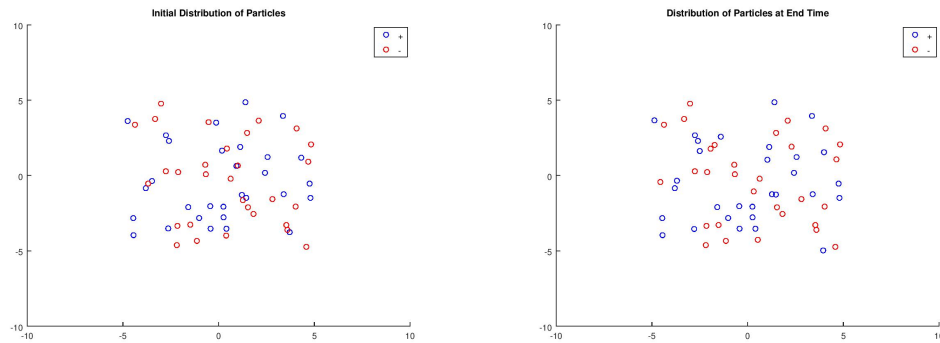


Figure 8: On the left, the initial distribution of agents for $|q_P| = |q_N| = 0.6$ in the first ODE model in two dimensions. 18 agents were dissatisfied. On the right, the end distribution of agents at $T = 20$ for $|q_P| = |q_N| = 0.6$. 0 agents were dissatisfied.

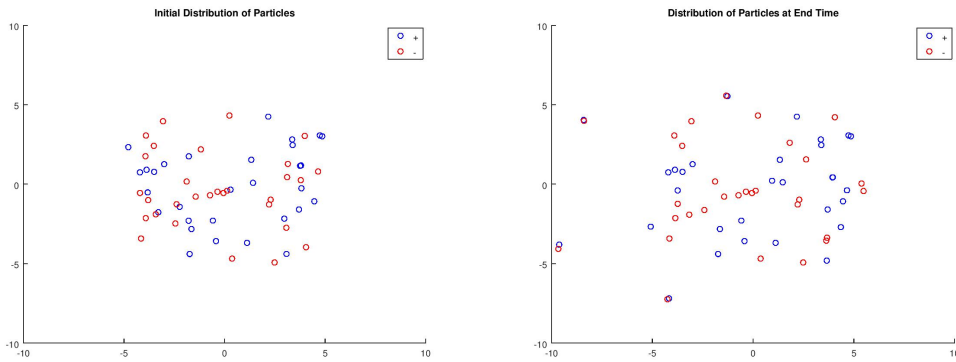


Figure 9: On the left, the initial distribution of agents for $|q_P| = |q_N| = 0.7$ in the first ODE model in two dimensions. 26 agents were dissatisfied. On the right, the end distribution of agents at $T = 20$ for $|q_P| = |q_N| = 0.7$. 9 agents were dissatisfied.

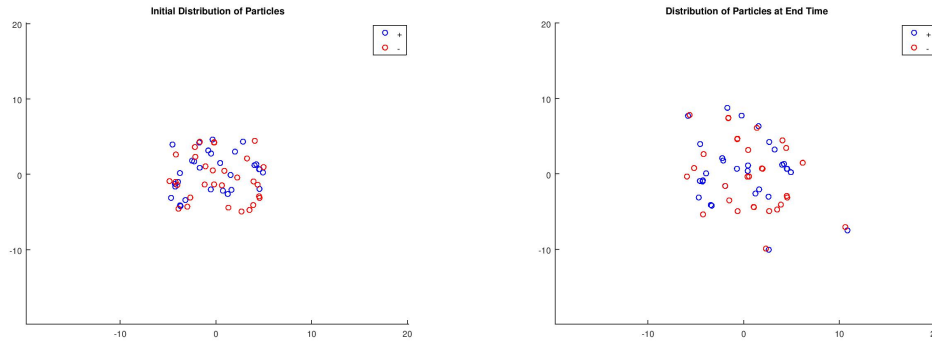


Figure 10: On the left, the initial distribution of agents for $|q_P| = |q_N| = 0.8$ in the first ODE model in two dimensions. 41 agents were dissatisfied. On the right, the end distribution of agents at $T = 20$ for $|q_P| = |q_N| = 0.8$. 15 agents were dissatisfied.

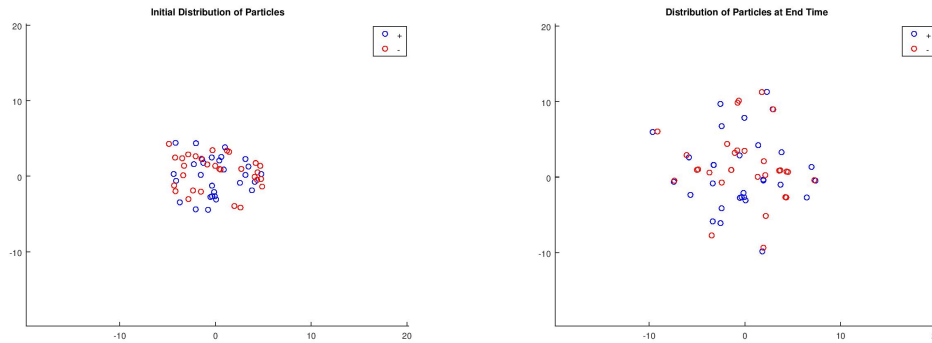


Figure 11: On the left, the initial distribution of agents for $|q_P| = |q_N| = 0.9$ in the first ODE model in two dimensions. 53 agents were dissatisfied. On the right, the end distribution of agents at $T = 20$ for $|q_P| = |q_N| = 0.9$. 30 agents were dissatisfied.

3.5 A Second ODE Model

A different model for segregation may be constructed by introducing the similarity function, $\chi_{|q_j|}(q_i)$, as a weight on the sums in the movement function, $\dot{x}_i = f_i$. The weight corresponds to the assumption that agents only pay attention to agents of the same similarity. Along with the weights, the order of subtraction is reversed in the function μ , representing the scenario where agents move towards agents that are more satisfied than themselves. The movement function is given by

$$\dot{x}_i = \alpha_i \left(\sum_{j=1}^N \psi(|x_i - x_j|) \chi_{|q_j|}(q_i) \mu(C(x_j) - C(x_i)) (x_j - x_i) \right) \Lambda_{|q_i|}(C(x_i)) \quad (15)$$

3.5.1 Simulations Of The Second ODE Model

A fourth-order Runge-Kutta method was used to solve the second ODE Model, (15), where agents were randomly uniformly dispersed over the interval $[-3, 3]$ for the one dimensional case and over $[-3, 3] \times [0, 3]$ in the two dimensional case. The following parameters were chosen: $N = 120$ agents with $k = 60$ positive and negative agents, time $T = 10$, step size for time of $h = 0.01$, $\alpha = 1$, $t = 2$, $\beta = 2$, $l = 1000$, and $c = 1000000$. Unlike the first ODE Model, almost every simulation reached a stopping point before $T = 10$, the segregation amongst the agents is more definitive, and the area over which the agents move tends to stay much closer to the initial area. As the threshold increases, the clusters become more defined. The number of clusters of agents at the end time in the second ODE Model tend to be lower than in the first.

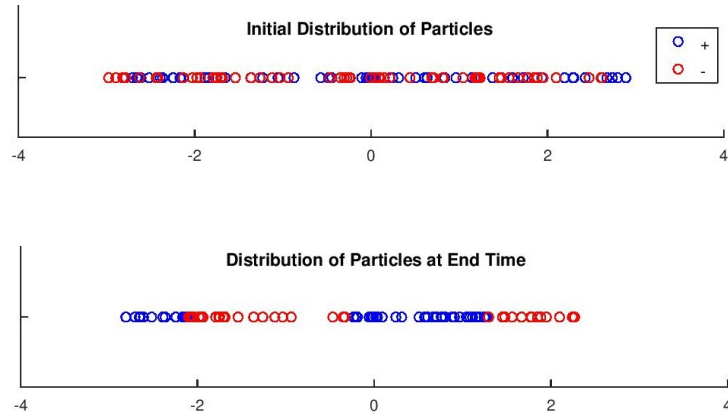


Figure 12: On the left, the initial distribution of agents with $|q_P| = |q_N| = 0.5$ in the second ODE model in one dimension. 49 agents were dissatisfied. On the right, the end distribution of agents with $T = 10$. 0 agents were dissatisfied.

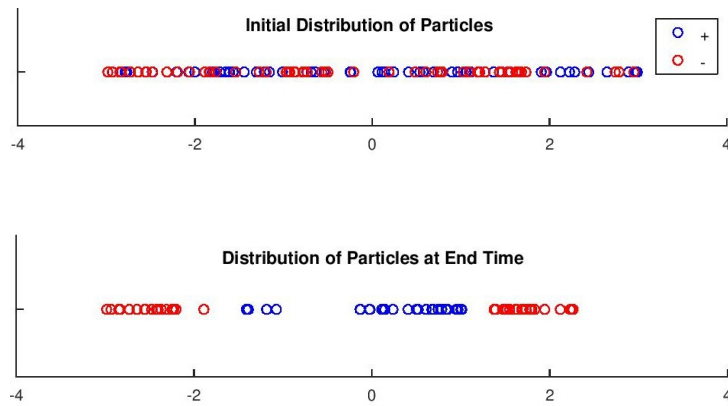


Figure 13: On the left, the initial distribution of agents with $|q_P| = |q_N| = 0.6$ in the second ODE model in one dimension. 105 agents were dissatisfied. On the right, the end distribution of agents with $T = 10$. 0 agents were dissatisfied.

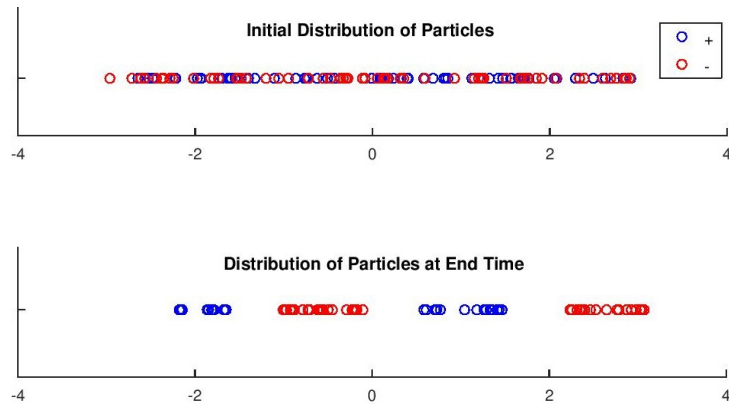


Figure 14: On the left, the initial distribution of agents with $|q_P| = |q_N| = 0.7$ in the second ODE model in one dimension. 120 agents were dissatisfied. On the right, the end distribution of agents with $T = 10$. 0 agents were dissatisfied.

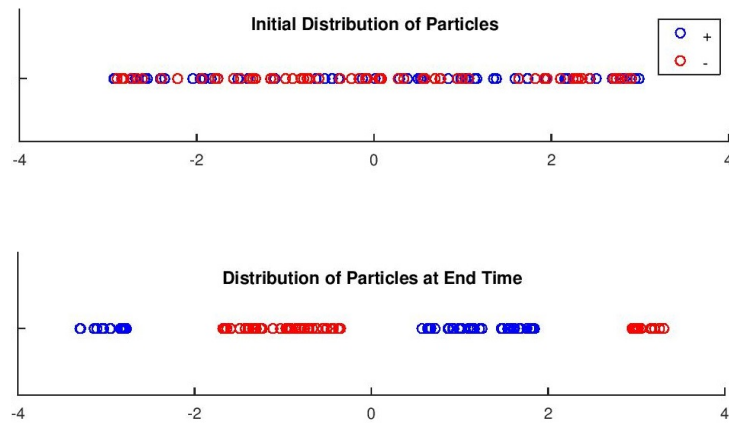


Figure 15: On the left, the initial distribution of agents with $|q_P| = |q_N| = 0.8$ in the second ODE model in one dimension. 120 agents were dissatisfied. On the right, the end distribution of agents with $T = 10$. 0 agents were dissatisfied.

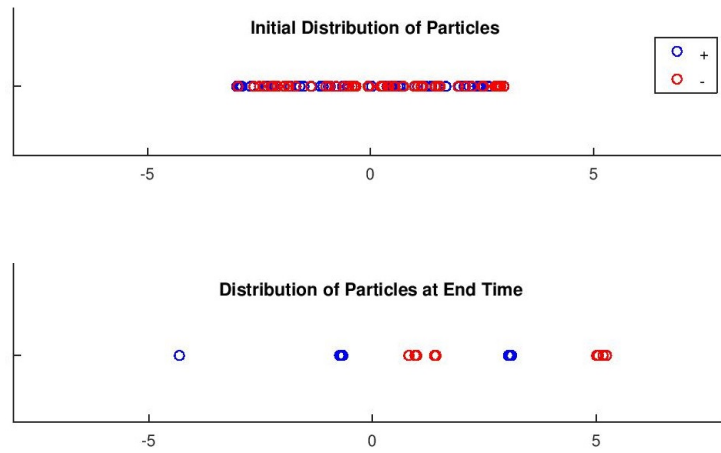


Figure 16: On the left, the initial distribution of agents with $|q_P| = |q_N| = 0.9$ in the second ODE model in one dimension. 120 agents were dissatisfied. On the right, the end distribution of agents with $T = 10$. 0 agents were dissatisfied.

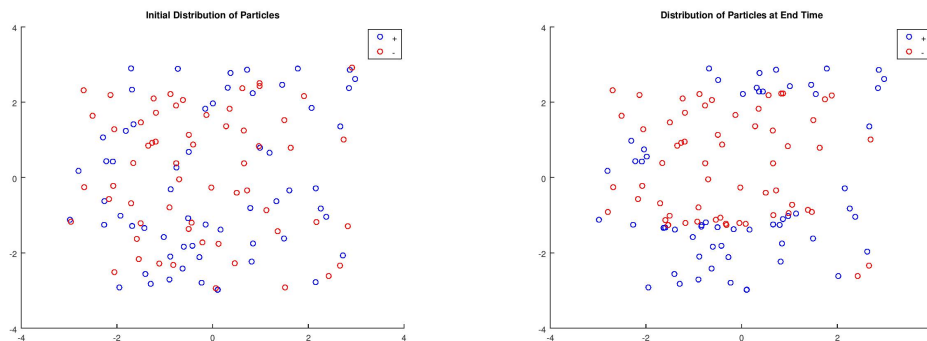


Figure 17: On the left, the initial distribution of agents with $|q_P| = |q_N| = 0.5$ in the second ODE model in two dimensions. 34 agents were dissatisfied. On the right, the end distribution of agents with $T = 10$. 0 agents were dissatisfied.

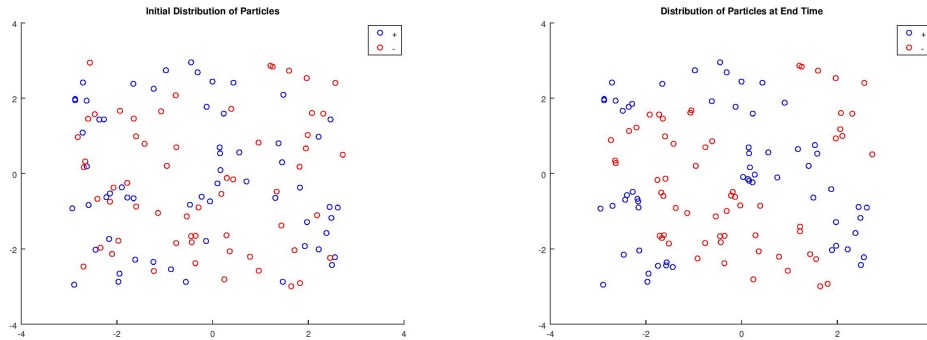


Figure 18: On the left, the initial distribution of agents with $|q_P| = |q_N| = 0.6$ in the second ODE model in two dimensions. 70 agents were dissatisfied. On the right, the end distribution of agents with $T = 10$. 0 agents were dissatisfied.

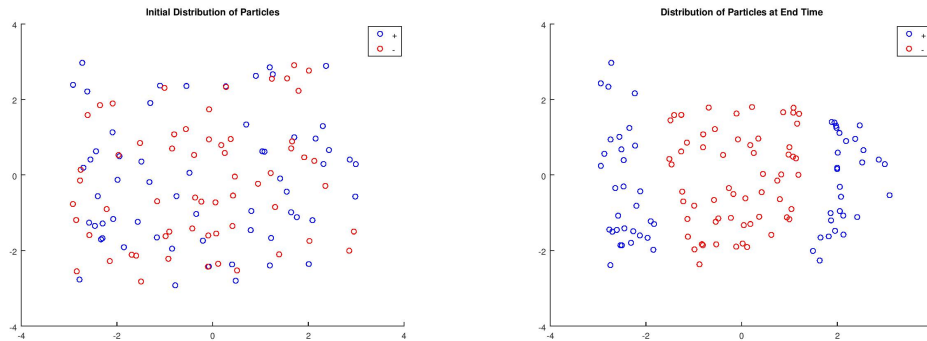


Figure 19: On the left, the initial distribution of agents with $|q_P| = |q_N| = 0.7$ in the second ODE model in two dimensions. 111 agents were dissatisfied. On the right, the end distribution of agents with $T = 10$. 0 agents were dissatisfied.

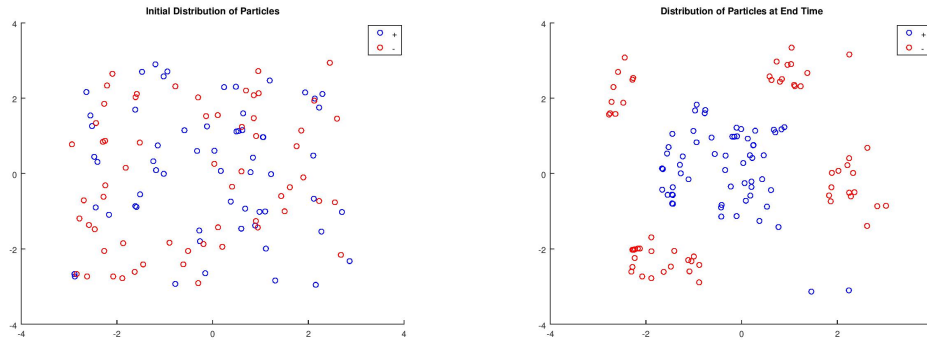


Figure 20: On the left, the initial distribution of agents with $|q_P| = |q_N| = 0.8$ in the second ODE model in two dimensions. 120 agents were dissatisfied. On the right, the end distribution of agents with $T = 10$. 0 agents were dissatisfied.

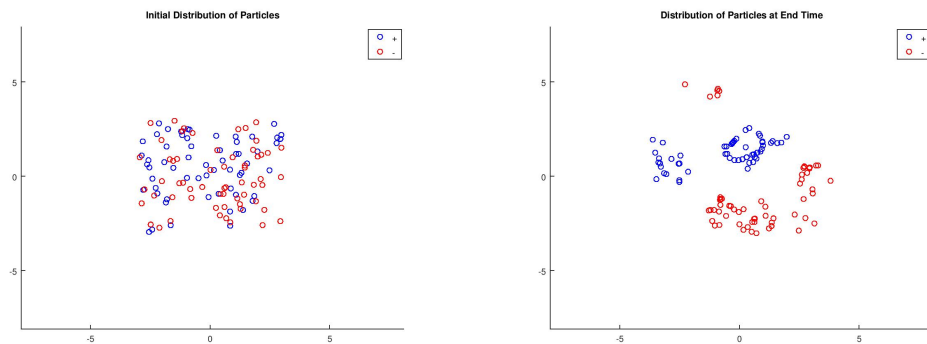


Figure 21: On the left, the initial distribution of agents with $|q_P| = |q_N| = 0.9$ in the second ODE model in two dimensions. 120 agents were dissatisfied. On the right, the end distribution of agents with $T = 10$. 0 agents were dissatisfied.

CHAPTER 4

Concluding Remarks

The concept of velocity alignment in flocking can provide a simple, powerful tool in the construction of new continuous models for social dynamics. It exhibits an ideal scenario where every agent cooperates through the same actions to achieve one unified goal. Since mathematical modeling often prefers simplicity, especially in the advent of new phenomena, one can view velocity alignment then as a starting point for model making in some areas in the social sciences. To adjust the functionality of velocity alignment equations with the intent of modeling a new phenomena only requires variations of the behavior in subpopulations of the larger conforming group. If the behavior of an agent relies on the population, then its behavior depends, directly or indirectly, on the cooperation of the masses. Otherwise, no social behavior occurs in the agent, yielding a distinct phenomena.

The Cucker-Smale Variant, (2), offers a way of departing the social aspects of a group from its geometry. The loosened adherence to the velocity alignment equation provides stronger control over the agents' configuration, allowing for a wider variety of applications in engineering, biology, and the social sciences. For example, the velocity alignment equation has been used to create the first and second ODE Models for segregation presented in Chapter 3. One can then define a differential equation that governs the change of the quality q_i over time, which would allow the system to model belief dynamics, politics, or business trends that take location into consideration. Introducing an additional function describing a distribution of resources could produce an economic or game-theoretic model. The theorems proven in Chapter 2 offer criteria for the occurrence of collective behavior as well as a tool

for modeling and machinery for analyzing the orientations of flocks, exhibited theoretically and in simulation by Theorem 2.6.

Finally, a number of fruitful propositions about the Particle Cucker-Smale Model, the Cucker-Smale Variant, and the Centered Cucker-Smale Variant may hold that have yet to be proven. Theorem 2.6 suggests that the introduction of a controller could form a new system in which $x_i(t)$ converges to $d_i(t)$ in finite time instead of asymptotically. This would allow us to replace the assumption that $\lim_{t \rightarrow \infty} d'_{ij}(t) = 0$ with a stronger condition allowing for agents to take on a configuration in constant non-converging motion. Such an insight could lead to applications in engineering that requires, for example, a swarm to assume an orientation with a time limit. The three systems may have a certain equivalence up to their influence functions given limitations on the spans of their spaces and by imposing a linear structure on \dot{x}_i , \dot{v}_i , and f_i . The physical intuition comes from realizing that drones cannot assume an orientation in a spatial dimension higher than three. Explicitly, no one can conceive of movement in 4-space and such a limitation suggests no one can try without aid. Such an equivalence could offer natural ways of crafting influence functions for maintaining desirable properties about the movement and orientation of the agents.

BIBLIOGRAPHY

- [1] C. Reynolds. *Flocks, herds and schools: A distributed behavioral model*. SIGGRAPH '87: Proceedings of the 14th Annual Conference on Computer Graphics and Interactive Techniques. 1987.
- [2] T. Vicsek, et. al, *Novel Type of Phase Transition in a System of Self-Driven Particles*. American Physical Society (APS). 1995.
- [3] F. Cucker, S. Smale, *Emergent Behavior in Flocks*, IEEE Transactions on Automatic Control. Vol 52. Issue: 5. pp 852- 862. 2007.
- [4] S.-Y. HA, E. Tadmor, *From Particle to Kinetic and Hydrodynamic Descriptions of Flocking*. arXiv:0806.2182. 2008.
- [5] T. Karper, A. Mellet, K. Trivisa, *Existence of Weak Solutions to Kinetic Flocking Models*. SIAM J. MATH. ANAL. Vol. 45, pp. 215-243. 2013.
- [6] J. Morales, J. Peszek, E. Tadmor. *Flocking with Short-Range Interactions*. arXiv:1812.03567. 2018.
- [7] Uri. Wilensky, William. Rand. *An Introduction to Agent-Based Modeling: Modeling Natural, Social, and Engineered Complex Systems with NetLogo*. MIT Press Cambridge, Massachusetts. 2015.
- [8] Thomas C. Schelling. *Dynamic Models of Segregation* Journal of Mathematical Sociology. Gordon and Breach Science Publishers. Vol 1, pp 143-186. 1971.
- [9] S. Pérez. *A Numerical Study for Collective Behaviour Models: From Microscopic to Macroscopic Models*. Undergraduate Research Opportunity Program Imperial College. 2015.

- [10] S.-Y. Ha, J.-G. Liu, *A Simple Proof of The Cucker-Smale Flocking Dynamics and Mean-Field Limit*. International Press. Commun. Math. Sci. Vol 7. No. 2, pp 297-325. 2009.
- [11] L. Perko. *Differential Equations and Dynamical Systems* 3rd ed. Springer-Verlag. New York, inc. 2001.

APPENDICES

APPENDIX A
THEOREMS

Theorem 1.8 (A Special Case of Grönwall's Inequality (Differential form))

Let $I = [t_0, t_1]$. Suppose $a : I \rightarrow \mathbb{R}$ and $b : I \rightarrow \mathbb{R}$ are continuous, and suppose $u : I \rightarrow \mathbb{R}$ is in $C^1(I)$ and satisfies

$$u'(t) \leq a(t)u(t) \quad \text{for } t \in I, \quad \text{and } u(t_0) = u_0.$$

Then

$$u(t) \leq u_0 e^{\int_{t_0}^t a(s) ds}$$

Various book present Grönwall's Inequality in its integral form, e.g. Perko [11]. Here, we prove a special case of Grönwall's Inequality in differential form.

Proof. Since $e^{\int_{t_0}^{t_1} a(s) ds} > 0$, we multiply both sides of the inequality to obtain

$$\begin{aligned} u(t) e^{-\int_{t_0}^t a(s) ds} &\leq a(t) u(t) e^{-\int_{t_0}^t a(s) ds} \\ u(t) e^{-\int_{t_0}^t a(s) ds} - a(t) u(t) e^{-\int_{t_0}^t a(s) ds} &\leq 0 \\ \frac{d}{dt} \left(u(t) e^{-\int_{t_0}^t a(s) ds} \right) &\leq 0 \end{aligned}$$

Integrating from t_0 to t then gives

$$\begin{aligned} u(t) e^{-\int_{t_0}^t a(s) ds} - u(t_0) e^{-\int_{t_0}^{t_0} a(s) ds} &\leq 0 \\ u(t) e^{-\int_{t_0}^t a(s) ds} &\leq u_0 \end{aligned}$$

$$u(t) \leq u_0 e^{\int_{t_0}^t a(s) ds}$$

□

Here is a special case of Lemma (2.2), followed by a proof of the second inequality as discussed in Chapter 2.

Lemma 1.9 *Let f_i be Lipschitz and (x, v) be any solution to the system (1). Then,*

$$\frac{d}{dt}X(t) \leq V(t) \tag{A.16}$$

$$\frac{d}{dt}V(t) \leq -K\psi(X(t))V(t) \tag{A.17}$$

where $X(t) = \max_{1 \leq i, j \leq N} |x_i(t) - x_j(t)|$ and $V(t) = \max_{1 \leq i, j \leq N} |v_i(t) - v_j(t)|$

The proof of the first inequality, (1.9), was proven in Chapter 1 in a more general setting. This section offers a proof of the second inequality, (1.9), based off of the proof found in Perez [9].

Proof. Assume i and j are so that $|v_i - v_j| = V(t)$. If $\psi(0) = 0$, then $\psi = 0$ over $[0, \infty)$ and the result is trivial. Let $\psi(0) > 0$. Since ψ is decreasing over $[0, \infty)$, let $\phi(r) = \frac{\psi(r)}{\psi(0)}$ and note that $0 \leq \phi(r) \leq 1$ for $r \in [0, \infty)$. Then

$$\begin{aligned} \frac{1}{2} \frac{d}{dt} |v_i - v_j|^2 &= (v_i - v_j) \cdot \left(\frac{d}{dt} v_i - \frac{d}{dt} v_j \right) \\ &= \psi(0)(v_i - v_j) \cdot \left(\frac{K}{N} \sum_{k=1}^N \phi(|x_i - x_k|)(v_k - v_i) - \frac{K}{N} \sum_{k=1}^N \phi(|x_j - x_k|)(v_k - v_j) \right) \end{aligned}$$

Then note

$$\begin{aligned} (v_i - v_j) \cdot (v_k - v_i) &= (v_i - v_j) \cdot ((v_k - v_j) + (v_j - v_i)) \\ &= (v_i - v_j) \cdot (v_k - v_j) + (v_i - v_j) \cdot (v_j - v_i) \end{aligned}$$

$$= (v_i - v_j) \cdot (v_k - v_j) - |v_i - v_j|^2 \leq 0$$

by choice of i and j . Since $0 < \phi \leq 1$ and $\phi(|x_k - x_i|) \geq \phi(X(t))$,

$$\phi(|x_k - x_i|)(v_i - v_j) \cdot (v_k - v_i) \leq \phi(X(t))(v_i - v_j) \cdot (v_k - v_i) \leq 0$$

Multiplying by $\frac{K}{N}\psi(0)$ and summing over k gives us that

$$\frac{K}{N} \sum_{k=1}^N \psi(|x_k - x_i|)(v_i - v_j) \cdot (v_k - v_i) \leq \frac{K}{N} \sum_{k=1}^N \psi(X(t))(v_i - v_j) \cdot (v_k - v_i) \leq 0$$

In a similar way, we obtain

$$-\frac{K}{N} \sum_{k=1}^N \psi(|x_k - x_j|)(v_i - v_j) \cdot (v_k - v_j) \leq -\frac{K}{N} \sum_{k=1}^N \psi(X(t))(v_i - v_j) \cdot (v_k - v_j) \leq 0$$

Thus,

$$\begin{aligned} \frac{d}{dt} \frac{1}{2} |v_i - v_j|^2 &= (v_i - v_j) \cdot \left(\frac{d}{dt} v_i - \frac{d}{dt} v_j \right) \\ &= (v_i - v_j) \cdot \left(\frac{K}{N} \sum_{k=1}^N \psi(|x_k - x_i|)(v_k - v_i) - \frac{K}{N} \sum_{k=1}^N \psi(|x_k - x_j|)(v_k - v_j) \right) \\ &\leq (v_i - v_j) \cdot \left(\frac{K}{N} \sum_{k=1}^N \psi(X(t))(v_k - v_i) - \frac{K}{N} \sum_{k=1}^N \psi(X(t))(v_k - v_j) \right) \\ &= \psi(X(t)) \frac{K}{N} (v_i - v_j) \cdot \left(\sum_{k=1}^N (v_k - v_i) - \sum_{k=1}^N (v_k - v_j) \right) \\ &= \psi(X(t)) \frac{K}{N} (v_i - v_j) \cdot \left(\sum_{k=1}^N (v_j - v_i) \right) \\ &= \psi(X(t)) \frac{K}{N} (v_i - v_j) \cdot (N(v_j - v_i)) \\ &= \psi(X(t)) K (v_i - v_j) \cdot (v_j - v_i) \\ &= -K \psi(X(t)) [V(t)]^2 \end{aligned}$$

by choice of i and j . However, $\frac{d}{dt} \frac{1}{2} |v_i - v_j|^2 = \frac{d}{dt} [V(t)]^2 = V(t) \frac{d}{dt} V(t)$. So,

$$\frac{d}{dt} V(t) \leq -K \psi(X(t)) V(t)$$

□

APPENDIX B

NOTATION

$|v|$:= A norm of vector v in \mathbb{R}^d .

r := An arbitrary number in \mathbb{R} or a subset of \mathbb{R} .

x := An arbitrary vector in \mathbb{R}^d or subset of \mathbb{R}^d .

x_i := Position vector of agent i in \mathbb{R}^d .

v_i := Velocity vector of agent i in \mathbb{R}^d .

q_i := Quality or qualities of agent i .

p_i := The particle i .

χ_r := The characteristic function over the interval $[0, r]$ for $r > 0$.

Λ_r := A corresponding bump function to χ_r whose support is the interval $[0, r]$.

\bar{x} := Arithmetic average of x over $1 \leq i \leq N$. Note: This is a vector.

\bar{r} := Arithmetic average of r over $1 \leq i \leq N$.

\dot{x} := Component-wise derivative of the vector function $x : \mathbb{R} \rightarrow \mathbb{R}^d$ with respect to time.

x' := Derivative of the scalar function $x : \mathbb{R} \rightarrow \mathbb{R}$ with respect to time.

∇_x := The gradient operator in components of x . e.g. for a vector $x_i \in \mathbb{R}^d$,

$$\nabla_x x_i = \left(\frac{\partial}{\partial x_{i1}} x_i, \frac{\partial}{\partial x_{i2}} x_i, \dots, \frac{\partial}{\partial x_{id}} x_i \right)$$

C_c^∞ := The set of functions $f : \mathbb{R} \rightarrow \mathbb{R}$ that have compact support and are infinitely differentiable.